Giant Spin-Orbit Induced Magnon Nonreciprocity in Ultrathin Ferromagnets

Khalil Zakeri * and Albrecht von Faber
Heisenberg Spin-dynamics Group, Physikalisches Institut, Karlsruhe Institute of Technology, Wolfgang-Gaede-Strasse 1, D-76131 Karlsruhe, Germany

(Received 9 May 2023; accepted 15 February 2024; published 21 March 2024)

The propagation characteristics of fermionic and bosonic quasiparticles determine the fundamental transport properties of solids and are of great technological relevance for designing logic devices. In particular, nonreciprocity, which describes that a quasiparticle flows preferably along a certain direction of a symmetry path, is an essential requirement to realize logic architectures, e.g., switches, diodes, transistors, etc. Here we introduce a mechanism, which leads to giant nonreciprocity of ultrafast terahertz magnons in ferromagnetic films with a large spin-orbit coupling. The mechanism is based on the competition between the exchange and spin-orbit scattering. We anticipate that the effect can be used to excite nonreciprocal or even unidirectional magnons in a large class of ultrathin films and nanostructures grown on substrates with a large spin-orbit coupling.

DOI: 10.1103/PhysRevLett.132.126702

In physics when the real or reciprocal space propagation of quasiparticles, e.g., electrons, photons, phonons, or magnons in a medium along a certain symmetry line depends on the direction, one speaks of nonreciprocity [1–3]. This property is the key ingredient for designing logic devices, which utilize these quasiparticles as carriers, such as rectifiers, switches, diodes, transistors, etc. In the emerging field of magnonics, which focuses on utilizing magnons, quanta of spin waves, for information processing, the magnon nonreciprocity is of special interest. Several magnon-based logic elements have been proposed based on this property [4–7]. Apart from the fact that in thin ferromagnetic films the classical dipolar Damon-Eschbach magnons are naturally nonreciprocal [8–11], there has been several proposals to generate nonreciprocal magnons in engineered structures. For instance, in structures with modified geometries [12–21], magnetic films with a significant Dzyaloshinskii-Moriya interaction (DMI) [22–26], coupled magnetic bilayers [27–31], systems with chiral spin Seebeck effect [32], magnon-fluxon coupled structures [33], or devices with a magnon Doppler shift [34,35], nonreciprocal magnons have been demonstrated. Most of these approaches are useful for low-frequency, long-wavelength magnons only. Since the speed of operation is an extremely important concept in magnonics, new approaches for exciting nonreciprocal high-frequency, terahertz (THz) magnons are highly in demand [25,36,37].

Here we introduce a mechanism, which leads to giant nonreciprocity of exchange-dominated ultrafast THz magnons in ultrathin ferromagnetic films having a large spin-orbit coupling (SOC), without influencing their frequency.

When a beam of electrons is scattered from a surface with a large SOC it can be polarized, since the scattering cross section becomes spin dependent. The polarization vector of the beam is transversal and is along the scattering plane's normal vector $\hat{\boldsymbol{n}}$, if the scattering plane is a mirror plane of the crystal [38–40]. Likewise, when a spin-polarized electron beam with a polarization vector parallel and antiparallel to $\hat{\boldsymbol{n}}$ is scattered from such a surface one expects a notable spin asymmetry, i.e., spin-orbit asymmetry (SOA) [38–40].

A spin asymmetry is also expected when a spin-polarized beam is scattered from a ferromagnetic surface with a spontaneous magnetization $\boldsymbol{M}$. The physical mechanism responsible for this "exchange asymmetry" (ExA) is the quantum mechanical exchange scattering process. Such a spin asymmetry reflects the local magnetic order and has been used to probe the surface magnetism [41,42]. Since in bulk $3d$ ferromagnets SOC is rather small, the observed spin asymmetry of electrons scattered from these surfaces is mainly of ExA type, caused by the exchange scattering process.

The situation becomes complex when ultrathin films of $3d$ ferromagnets are grown on heavy-element metallic substrates. In such a case SOC can be significantly large and can dominate the spin asymmetry of the spin-polarized electrons scattered from such surfaces. The mechanisms behind SOA and ExA are well known for elastically scattered electrons [38–40]. However, little is known for the case in which electrons show an apparent energy loss (or gain) during the scattering event [43,44]. Spin-polarized electrons can be used to excite collective spin excitations at surfaces, e.g., magnons [45–47]. The main physical mechanism behind the magnon excitation process is the exchange scattering process in which an electron with the spin parallel to $\boldsymbol{M}$ is scattered to an electron with the opposite spin (see Supplemental Note I of [48]). It is obvious that the coexistence of SOA and ExA would influence the magnon

0031-9007/24/132(12)/126702(7)

excitation process in systems exhibiting a large SOC. We will demonstrate that a strong competition between SOA and ExA leads to a substantial THz magnon nonreciprocity. The effect is significant and can even lead to unidirectional magnons for a certain range of magnon wave vector $\boldsymbol{Q}$. Such an effect may be used to realize new functionalities in magnonic devices, which utilize ultrafast exchange-dominated THz magnons.

The experiments were performed on an ultrathin Co layer, with the thickness of 1.8 atomic layers, epitaxially grown on the Ir(001) surface. The magnons were excited and probed by means of spin-polarized high-resolution electron energy-loss spectroscopy (SPHREELS). The incoming spin-polarized electron beam excites the magnons and the outgoing beam carries all the information regarding the excitations left behind e.g., energy (frequency), wave vector (wavelength), and lifetime [47]. All the experiments were performed at room temperature. The scattering geometry is schematically shown in the inset of Fig. 1. A monochromatic spin-polarized electron beam with the spin-polarization vector $\boldsymbol{P}$ parallel and antiparallel to the scattering plane's normal vector $\hat{\boldsymbol{n}}$ is scattered from the surface. The energy distribution of the scattered electrons is recorded with respect to the direction of $\boldsymbol{P}$. Conventionally, the experiments are performed for a certain magnetization direction, e.g., parallel to $\hat{\boldsymbol{n}}$. Here, in order to address the SOC-related phenomena the spectra were recorded for two possible directions of $\boldsymbol{M}$ parallel and antiparallel to $\hat{\boldsymbol{n}}$. This results in four partial intensity spectra $I_{\mu\nu}$, where the subscript μ represents the direction of $\boldsymbol{M}$ and ν represents that of $\boldsymbol{P}$. For instance $I_{\downarrow\downarrow}$ ($I_{\uparrow\uparrow}$) denotes the partial intensity spectrum in which the direction of both $\boldsymbol{M}$ and $\boldsymbol{P}$ is parallel (antiparallel) to $\hat{\boldsymbol{n}}$. Likewise, $I_{\downarrow\uparrow}$ ($I_{\uparrow\downarrow}$) denotes the partial intensity spectrum when $\boldsymbol{M}$ is parallel (antiparallel) to $\hat{\boldsymbol{n}}$ and $\boldsymbol{P}$ is antiparallel (parallel) to $\hat{\boldsymbol{n}}$. In the spectra shown in Fig. 1(a), first the sample was magnetized along the $[1\bar{1}0]$-direction, which indicates $\mu = \downarrow$. Then $I_{\downarrow\downarrow}$ and $I_{\downarrow\uparrow}$ were recorded. The difference spectrum denoted as $I_{\downarrow\downarrow} - I_{\downarrow\uparrow}$ represents a spin-flip excitation, i.e., a magnon. The magnon excitation is mediated by the exchange mechanism in which a spin-down electron (an electron with the spin parallel to $\boldsymbol{M}$) is scattered to an electron of spin-up character (an electron with the spin antiparallel to $\boldsymbol{M}$), transferring $1\hbar$ angular momentum into the sample ($\hbar$ is the reduced Planck's constant, see Supplemental Note I of the Supplemental Material [48]). Note that the spin-up and spin-down are defined with respect to the direction of majority and minority spin states of the sample. Hence, in the absence of SOC one expects to observe an identical signal when $\boldsymbol{M}$ is switched to the opposite direction, i.e., $[\bar{1}10]$.

Since the direction of $\boldsymbol{M}$ is reversed with respect to the initial direction, the sign of the difference spectrum $I_{\uparrow\downarrow} - I_{\uparrow\uparrow}$ should be opposite to that of $I_{\downarrow\downarrow} - I_{\downarrow\uparrow}$. In Fig. 1(b) we show the spectra recorded for $\boldsymbol{M}\|[\bar{1}10]$. Since magnons are always excited by spin-down electrons, one must observe a negative difference spectrum, as observed in Fig. 1(b). The small peak at about 53 meV is caused by the vibrational excitations of adsorbates and

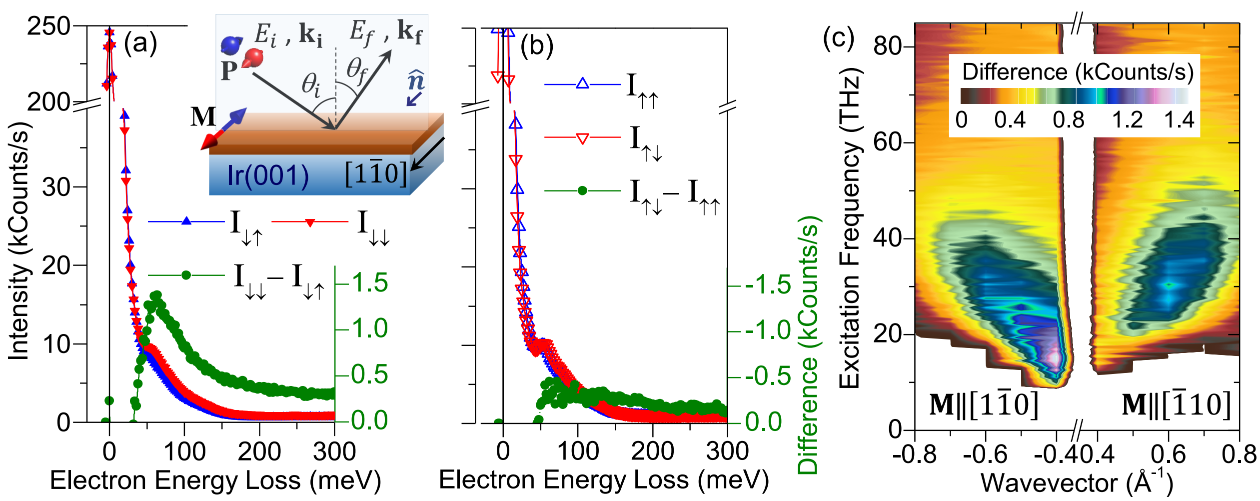

FIG. 1. SPHREEL spectra recorded at the wave vector of $|\boldsymbol{Q}| = -0.4$ Å^{-1}, using an incident energy of $E_i = 9$ eV. The partial intensity spectra are denoted by $I_{\mu\nu}$, where the subscripts μ and ν represent the direction of $\boldsymbol{M}$ and that of the spin polarization vector $\boldsymbol{P}$, respectively. The difference spectra are shown by the green color, which represent the magnon signal. The results for $\boldsymbol{M}\|[1\bar{1}0]$ are shown in (a) and those for $\boldsymbol{M}\|[\bar{1}10]$ are shown in (b), representing magnons with propagation direction along the [110] and $[\bar{1}\,\bar{1}\,0]$ direction, respectively. A schematic representation of the scattering geometry is shown in the inset. (c) The frequency-momentum map of the difference spectra $|I_{\downarrow\downarrow} - I_{\downarrow\uparrow}|$ or $|I_{\uparrow\downarrow} - I_{\uparrow\uparrow}|$ recorded for the two opposite directions of the magnetization, i.e., $\boldsymbol{M}\|[\bar{1}10]$ and $\boldsymbol{M}\|[1\bar{1}0]$. The color represents also the amplitude of coherently excited magnons. Data with the positive (negative) value of wave vector indicate the cases for which $\boldsymbol{M}\|[1\bar{1}0]$ ($\boldsymbol{M}\|[\bar{1}10]$) and the propagation direction along the [110] ($[\bar{1}\,\bar{1}\,0]$) direction.

does not show any dependence neither on the spin orientation of the electron beam nor on the direction of $\boldsymbol{M}$. The magnon signal appears as a satellite at about 66 meV. The surprising result is that the amplitude of the difference spectrum is largely suppressed. In ferromagnets, the time-reversal symmetry $\mathcal{T}$ is broken. Since reversing the sample magnetization is equivalent to a time-inversion experiment, the measurements performed for two opposite directions of $\boldsymbol{M}$ are equivalent to magnons propagating along opposite directions, perpendicular to $\boldsymbol{M}$. Comparing Figs. 1(a) and 1(b) reveals that the magnons with the propagation direction along [110] and $[\bar{1}\,\bar{1}\,0]$ possess very different excitation amplitudes. Hereafter we refer to this observation as magnon nonreciprocity, reflecting the nonreciprocal behavior of the amplitude of coherently excited magnons.

In order to answer the question whether this magnon nonreciprocity is present for magnons having different wave vectors, we performed the same experiments for different values of $|\boldsymbol{Q}|$ and the results are summarized in Fig. 1(c). The total scattering angle $\theta_0 = \theta_i + \theta_f = 80°$ was kept unchanged, in order to avoid unwanted effects [48]. The magnons with positive (negative) values of $|\boldsymbol{Q}|$ represent the cases in which $\boldsymbol{M}\|[1\bar{1}0]$ ($\boldsymbol{M}\|[\bar{1}10]$) and the propagation direction is along the [110] ($[\bar{1}\,\bar{1}\,0]$) direction. The magnon amplitude is encoded in the color map, where the quantity $|I_{\downarrow\downarrow} - I_{\downarrow\uparrow}|$ ($|I_{\uparrow\downarrow} - I_{\uparrow\uparrow}|$) is displayed. Figure 1(c) clearly indicates that the magnon nonreciprocity is significant at the low wave vector regime, in particular for $|\boldsymbol{Q}| \approx -0.4 \pm 0.1$ Å^{-1}, and becomes less significant at larger wave vectors. We note that a significant DMI [49,50] can lead to a magnon nonreciprocity [22,26,51–53]. The DMI-induced energy asymmetry for this particular wave vector is on the order of 1 meV (0.24 THz) or less [54]. The observed huge asymmetry in the magnon amplitude cannot be attributed to the DMI.

To visualize the dynamics of the magnons with opposite propagation directions, we constructed the magnon wave packets in real time and space (see Supplemental Note II and Supplemental Movie [48]). The results indicate that the two magnon wave packets exhibit very different dynamics but nearly the same frequency.

In order to shed light on the origin of this giant magnon nonreciprocity we investigated the spin asymmetry of the electrons scattered from this surface in great detail. Figure 2(a) shows the spin asymmetry recorded for the elastic scattering as a function of the incident beam energy E_i. The results are shown for four different cases: (i) the partial spin asymmetry for $\boldsymbol{M}\|[1\bar{1}0]$ defined as $A_{\boldsymbol{M}\|[1\bar{1}0]} = (I_{\downarrow\downarrow} - I_{\downarrow\uparrow})/(I_{\downarrow\downarrow} + I_{\downarrow\uparrow})$, (ii) the partial spin asymmetry for $\boldsymbol{M}\|[\bar{1}10] A_{\boldsymbol{M}\|[\bar{1}10]} = (I_{\uparrow\downarrow} - I_{\uparrow\uparrow})/(I_{\uparrow\downarrow} + I_{\uparrow\uparrow})$, (iii) ExA $A_{\mathrm{Ex}} = (I_{\downarrow\downarrow} - I_{\downarrow\uparrow} - I_{\uparrow\downarrow} + I_{\uparrow\uparrow})/(I_{\downarrow\downarrow} + I_{\downarrow\uparrow} + I_{\uparrow\downarrow} + I_{\uparrow\uparrow}) \approx (1/2)(A_{\vec{M}\|[1\bar{1}0]} - A_{\vec{M}\|[\bar{1}10]})$, and (iv) SOA $A_{\mathrm{SO}} = (I_{\downarrow\downarrow} - I_{\uparrow\uparrow} + I_{\uparrow\downarrow} - I_{\downarrow\uparrow})/(I_{\downarrow\downarrow} + I_{\downarrow\uparrow} + I_{\uparrow\downarrow} + I_{\uparrow\uparrow}) \approx (1/2)(A_{\vec{M}\|[1\bar{1}0]} + A_{\vec{M}\|[\bar{1}10]})$. We note that in order to separate the ExA and SOA

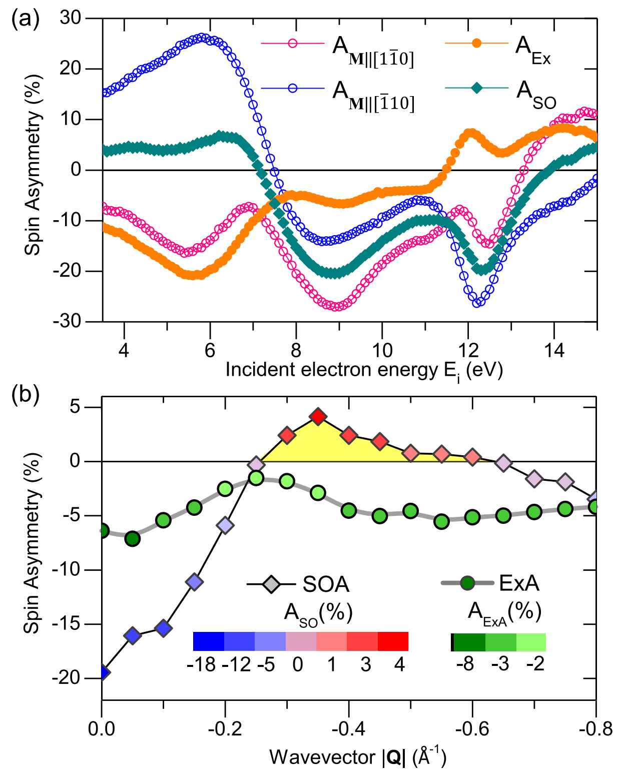

FIG. 2. (a) Different contributions to the spin asymmetry of elastically scattered electrons ($|\boldsymbol{Q}| = 0$) versus the incident beam energy E_i, as defined in the text. (b) The spin-orbit A_{SO} and exchange A_{Ex} asymmetry as a function of the wave vector, recorded for the incident energy of $E_i = 9$ eV. The shaded area in (b) highlights the region of wave vector for which SOA favors the magnon excitations process.

we assume that the interference between these two is negligible. This is a good assumption for the measured range of E_i. The important outcome of this investigation is that both ExA and SOA are substantially large and exhibit a strong dependence on E_i. More importantly, SOA is unexpectedly large and for 8 eV $< E_i <$ 14 eV overcomes ExA. This can have very important consequences on the magnon excitation process, when electrons with an incident energy in this range are used (see Supplemental Note I of [48]). The results presented in Fig. 2(a) were obtained for the elastic part of the scattering. However, one has to consider the following two important points. (i) The elastic and inelastic scattering are mutually interconnected, meaning that if spin-orbit scattering is significant in the elastic channel one would expect also a large contribution in the inelastic channel [44,55]. (ii) The magnon excitation is mediated by the quantum mechanical exchange process, in which an electron of minority spin character occupies an empty state above the Fermi-level of the system and an electron of majority spin character leaves the sample from an occupied state below the Fermi-level [47,56,66–68]. In spite of the fact that the magnon excitation peak appears in the inelastic (energy-loss) part of the spectrum, the excitation process is not a conventional inelastic process. Note that an inelastic scattering process is observed in the inelastic neutron or photon scattering experiments, where the scattering particles are truly inelastically scattered. In SPHREELS the apparent energy loss of the electron is due to the fact that the scattered electron stems from a lower energy state of the solid (see Refs. [46,47] and also Supplemental Note I of [48]). Based on the above mentioned arguments one would conclude that a competition between the large spin-orbit scattering and the exchange scattering plays a decisive role in the magnon excitation process and consequently on the observed magnon nonreciprocity. For $\boldsymbol{M}\|[1\bar{1}0]$, $\boldsymbol{Q}\|[110]$, it would enhance the excitation cross section and for $\boldsymbol{M}\|[\bar{1}10]$, $\boldsymbol{Q}\|[\bar{1}\,\bar{1}\,0]$, it would suppress the cross section. In other words, the chiral nature of SOC either hinders or facilitates the magnon excitations by the injected electron, depending on the relative orientation of the spin of the electron and the magnetization direction.

An important consideration is that both ExA and SOA depend on the scattering angles. Hence, when recording the spectra for different values of $|\boldsymbol{Q}|$ these quantities can be very different and may even undergo a sign reversal. In order to address this point we measured ExA and SOA as a function of $|\boldsymbol{Q}|$. The results for the incident energy of $E_i = 9$ eV are summarized in Fig. 2(b). The choice of $E_i = 9$ eV is based on the fact that at this energy the SOA is at a maximum. As it is clearly apparent, although ExA shows variations with $|\boldsymbol{Q}|$ and undergoes a minimum near $|\boldsymbol{Q}| \approx -0.25$ Å^{-1}, it always remains negative. In contrast, SOA exhibits drastic changes as $|\boldsymbol{Q}|$ increases. It even changes the sign from negative to positive at $|\boldsymbol{Q}| \approx -0.25$ Å^{-1}. For wave vectors between -0.25 and -0.5 Å^{-1} the opposite sign of A_{SO} with respect to that of A_{Ex} leads to an enhancement of the total spin asymmetry (larger probability of spin-down to spin-up scattering), which in turn is a measure of the magnons' excitation cross section. Hence for one magnetization direction, i.e., $\boldsymbol{M}\|[1\bar{1}0]$ and $\boldsymbol{Q}\|[110]$, the excitation cross section is enhanced. Consequently, for the other magnetization direction, i.e., $\boldsymbol{M}\|[\bar{1}10]$ and $\boldsymbol{Q}\|[\bar{1}\,\bar{1}\,0]$, the cross section is suppressed.

Unfortunately, a microscopic theory which can account for all the processes during the SPHREELS experiments from magnetic surfaces does not currently exist. However, one possible way to verify that the observed magnon nonreciprocity is due to the competition between ExA and SOA would be to simulate the experimental data using the dipolar scattering theory. An important contribution to include is the SOC during the scattering process. Luckily such a theory has been recently developed for nonmagnetic surfaces [44]. Simulations based on the dipolar scattering theory including SOC can reproduce the experimental results and explain the observed magnon nonreciprocity (see Supplemental Note III for details [48]). We calculated the magnon nonreciprocity, defined as the ratio of the amplitudes of the coherent magnon wave packets with the same eigenfrequency and wave vector but propagating along opposite directions ([110] and $[\bar{1}\,\bar{1}\,0]$). The results are summarized in Fig. 3 and are compared to those of the experiment. The results clearly indicate that the observed magnon nonreciprocity is a consequence of the strong competition between ExA and SOA.

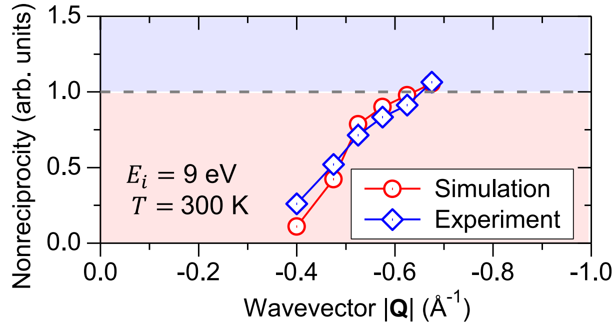

FIG. 3. The magnon nonreciprocity defined as the ratio of the amplitudes of the coherent magnon wave packets with the same eigenfrequency and wave vector but propagating along opposite directions ([110] and $[\bar{1}\,\bar{1}\,0]$). For the case that the nonreciprocity is equal to the unity the wave packets possess identical amplitudes and are perfectly reciprocal. Zero represents the unidirectional case.

The observed phenomenon is not limited to the present system. Although weaker, it should also be present in other SPHREELS experiments reported earlier [22,23,26,69] (see Supplemental Note III of [48]). We anticipate that it can take place in many other ferromagnetic thin films, heterostructures and nanostructures grown on heavy-element substrates or in heterostructures with a large SOC [70], e.g., magnetic structures grown on topological insulators [57] or two-dimensional van der Waals material [71–73], magnetic iridates [74], perovskite heterostructures [75], etc. The effect shall be observed by the laser [76,77] or transport based [78–84] excitation schemes, facilitating its integration in the current magnon-based technologies.

In conclusion, we demonstrated that the presence of a large SOC leads to nonreciprocal THz magnon amplitudes in ultrathin films. The nonreciprocity is understood based on the competition between two fundamental scattering mechanisms, namely, spin-orbit and exchange scattering mechanisms. Because of the large SOC, the spin-orbit scattering is significantly large and, under some circumstances, can overcome the exchange scattering mechanism. Combined with the fact that in ferromagnets $\mathcal{T}$ is broken, the spin-orbit scattering can either enhance or suppress the cross section of magnon excitations, when the magnons are excited by electrons. Hence, the amplitude of coherently excited magnons becomes dependent on the direction of static magnetization. The effect can be utilized to excite nonreciprocal magnons, having the same magnitude of wave vector and frequency, in ultrathin magnetic films and nanostructures grown on heavy-element substrates or even in more complex heterostructures with a large SOC. The effect is not restricted to the scattering experiments and must also be present in the transport based tunneling experiments, in which a spin-polarized current is used to excite magnons in tunneling magnetoresistance type of devices [78–84].

Financial support by the Deutsche Forschungsgemeinschaft (DFG) through the DFG Grants No. ZA 902/7-1, No. ZA 902/8-1 and No. ZA 902/5-1 and also the Heisenberg Programme ZA 902/3-1 and ZA 902/6-1 is acknowledged. K. Z. thanks the Physikalisches Institut for hosting the group and providing the necessary infrastructure.

*khalil.zakeri@partner.kit.edu

[1] L. Feng, M. Ayache, J. Huang, Y.-L. Xu, M.-H. Lu, Y.-F. Chen, Y. Fainman, and A. Scherer, Nonreciprocal light propagation in a silicon photonic circuit, Science **333**, 729 (2011).

[2] H. Ramezani, P. K. Jha, Y. Wang, and X. Zhang, Nonreciprocal localization of photons, Phys. Rev. Lett. **120**, 043901 (2018).

[3] M. Xu, K. Yamamoto, J. Puebla, K. Baumgaertl, B. Rana, K. Miura, H. Takahashi, D. Grundler, S. Maekawa, and Y. Otani, Nonreciprocal surface acoustic wave propagation via magneto-rotation coupling, Sci. Adv. **6**, eabb1724 (2020).

[4] V. V. Kruglyak, S. O. Demokritov, and D. Grundler, Magnonics, J. Phys. D **43**, 264001 (2010).

[5] S. Demokritov and A. Slavin, Magnonics: From fundamentals to applications, *Topics in Applied Physics* (Springer Berlin Heidelberg, Berlin, Heidelberg, 2012).

[6] A. V. Chumak, A. A. Serga, and B. Hillebrands, Magnon transistor for all-magnon data processing, Nat. Commun. **5**, 4700 (2014).

[7] A. V. Chumak, V. I. Vasyuchka, A. A. Serga, and B. Hillebrands, Magnon spintronics, Nat. Phys. **11**, 453 (2015).

[8] R. W. Damon and J. R. Eshbach, Magnetostatic modes of a ferromagnet slab, J. Phys. Chem. Solids **19**, 308 (1961).

[9] P. Grünberg, Light scattering from magnetic surface excitations, Prog. Surf. Sci. **18**, 1 (1985).

[10] K. Sekiguchi, K. Yamada, S. M. Seo, K. J. Lee, D. Chiba, K. Kobayashi, and T. Ono, Nonreciprocal emission of spin-wave packet in FeNi film, Appl. Phys. Lett. **97**, 022508 (2010).

[11] O. Gladii, M. Haidar, Y. Henry, M. Kostylev, and M. Bailleul, Frequency nonreciprocity of surface spin wave in permalloy thin films, Phys. Rev. B **93**, 054430 (2016).

[12] P. K. Amiri, B. Rejaei, M. Vroubel, and Y. Zhuang, Nonreciprocal spin wave spectroscopy of thin Ni–Fe stripes, Appl. Phys. Lett. **91**, 062502 (2007).

[13] T. Schneider, A. A. Serga, T. Neumann, B. Hillebrands, and M. P. Kostylev, Phase reciprocity of spin-wave excitation by a microstrip antenna, Phys. Rev. B **77**, 214411 (2008).

[14] M. Mruczkiewicz, M. Krawczyk, G. Gubbiotti, S. Tacchi, Y. A. Filimonov, D. V. Kalyabin, I. V. Lisenkov, and S. A. Nikitov, Nonreciprocity of spin waves in metallized magnonic crystal, New J. Phys. **15**, 113023 (2013).

[15] V. E. Demidov and S. O. Demokritov, Magnonic waveguides studied by microfocus brillouin light scattering, IEEE Trans. Magn. **51**, 1 (2015).

[16] J. A. Otálora, M. Yan, H. Schultheiss, R. Hertel, and A. Kákay, Curvature-induced asymmetric spin-wave dispersion, Phys. Rev. Lett. **117**, 227203 (2016).

[17] M. Mruczkiewicz, P. Graczyk, P. Lupo, A. Adeyeye, G. Gubbiotti, and M. Krawczyk, Spin-wave nonreciprocity and magnonic band structure in a thin permalloy film induced by dynamical coupling with an array of Ni stripes, Phys. Rev. B **96**, 104411 (2017).

[18] M. Madami, Y. Khivintsev, G. Gubbiotti, G. Dudko, A. Kozhevnikov, V. Sakharov, A. Stal'makhov, A. Khitun, and Y. Filimonov, Nonreciprocity of backward volume spin wave beams excited by the curved focusing transducer, Appl. Phys. Lett. **113**, 152403 (2018).

[19] J. Chen, T. Yu, C. Liu, T. Liu, M. Madami, K. Shen, J. Zhang, S. Tu, M. S. Alam, K. Xia, M. Wu, G. Gubbiotti, Y. M. Blanter, G. E. W. Bauer, and H. Yu, Excitation of unidirectional exchange spin waves by a nanoscale magnetic grating, Phys. Rev. B **100**, 104427 (2019).

[20] B. Heinz, Q. Wang, M. Schneider, E. Weiß, A. Lentfert, B. Lägel, T. Brächer, C. Dubs, O. V. Dobrovolskiy, P. Pirro, and A. V. Chumak, Long-range spin-wave propagation in transversely magnetized nano-scaled conduits, Appl. Phys. Lett. **118**, 132406 (2021).

[21] M. M. Salazar-Cardona, L. Körber, H. Schultheiss, K. Lenz, A. Thomas, K. Nielsch, A. Kákay, and J. A. Otálora, Nonreciprocity of spin waves in magnetic nanotubes with helical equilibrium magnetization, Appl. Phys. Lett. **118**, 262411 (2021).

[22] K. Zakeri, Y. Zhang, J. Prokop, T.-H. Chuang, N. Sakr, W. X. Tang, and J. Kirschner, Asymmetric spin-wave dispersion on Fe(110): Direct evidence of the Dzyaloshinskii-Moriya interaction, Phys. Rev. Lett. **104**, 137203 (2010).

[23] K. Zakeri, Y. Zhang, T.-H. Chuang, and J. Kirschner, Magnon lifetimes on the Fe(110) surface: The role of spin-orbit coupling, Phys. Rev. Lett. **108**, 197205 (2012).

[24] A. Giordano, R. Verba, R. Zivieri, A. Laudani, V. Puliafito, G. Gubbiotti, R. Tomasello, G. Siracusano, B. Azzerboni, M. Carpentieri, A. Slavin, and G. Finocchio, Spin-hall nano-oscillator with oblique magnetization and Dzyaloshinskii-Moriya interaction as generator of skyrmions and nonreciprocal spin-waves, Sci. Rep. **6**, 36020 (2016).

[25] K. Zakeri, Terahertz magnonics: Feasibility of using terahertz magnons for information processing, Physica (Amsterdam) **549C**, 164 (2018).

[26] S. Tsurkan and K. Zakeri, Giant Dzyaloshinskii-Moriya interaction in epitaxial Co/Fe bilayers with C_{2v} symmetry, Phys. Rev. B **102**, 060406(R) (2020).

[27] R. A. Gallardo, T. Schneider, A. K. Chaurasiya, A. Oelschlägel, S. S. P. K. Arekapudi, A. Roldán-Molina, R. Hübner, K. Lenz, A. Barman, J. Fassbender, J. Lindner, O. Hellwig, and P. Landeros, Reconfigurable spin-wave nonreciprocity induced by dipolar interaction in a coupled ferromagnetic bilayer, Phys. Rev. Appl. **12**, 034012 (2019).

[28] M. Ishibashi, Y. Shiota, T. Li, S. Funada, T. Moriyama, and T. Ono, Switchable giant nonreciprocal frequency shift of propagating spin waves in synthetic antiferromagnets, Sci. Adv. **6**, eaaz6931 (2020).

[29] J. Han, Y. Fan, B. C. McGoldrick, J. Finley, J. T. Hou, P. Zhang, and L. Liu, Nonreciprocal transmission of incoherent magnons with asymmetric diffusion length, Nano Lett. **21**, 7037 (2021).

[30] K. Szulc, S. Mendisch, M. Mruczkiewicz, F. Casoli, M. Becherer, and G. Gubbiotti, Nonreciprocal spin-wave dynamics in Pt/Co/W/Co/Pt multilayers, Phys. Rev. B **103**, 134404 (2021).

[31] O. Gladii, R. Salikhov, O. Hellwig, H. Schultheiss, J. Lindner, and R. A. Gallardo, Spin-wave nonreciprocity at the spin-flop transition region in synthetic antiferromagnets, Phys. Rev. B **107**, 104419 (2023).

[32] T. Yu, Y. M. Blanter, and G. E. W. Bauer, Chiral pumping of spin waves, Phys. Rev. Lett. **123**, 247202 (2019).

[33] O. V. Dobrovolskiy and A. V. Chumak, Nonreciprocal magnon fluxonics upon ferromagnet/superconductor hybrids, J. Magn. Magn. Mater. **543**, 168633 (2022).

[34] V. Vlaminck and M. Bailleul, Current-induced spin-wave Doppler shift, Science **322**, 410 (2008).

[35] A. V. Chumak, P. Dhagat, A. Jander, A. A. Serga, and B. Hillebrands, Reverse Doppler effect of magnons with negative group velocity scattered from a moving bragg grating, Phys. Rev. B **81**, 140404(R) (2010).

[36] B. Lenk, H. Ulrichs, F. Garbs, and M. Münzenberg, The building blocks of magnonics, Phys. Rep. **507**, 107 (2011).

[37] K. Zakeri, Magnonic crystals: Towards terahertz frequencies, J. Phys. Condens. Matter **32**, 363001 (2020).

[38] G. C. Wang, B. I. Dunlap, R. J. Celotta, and D. T. Pierce, Symmetry in low-energy-polarized-electron diffraction, Phys. Rev. Lett. **42**, 1349 (1979).

[39] J. Kirschner, *Polarized Electrons at Surfaces*, 1st ed., Springer Tracts in Modern Physics Vol. 106 (Springer, Berlin Heidelberg, 1985), pp. 1–160.

[40] R. Feder, Principles and theory of electron scattering and photoemission, in *Polarized Electrons in Surface Physics* (World Scientific, Singapore, 1986), pp. 125–241.

[41] U. Gradmann and S. F. Alvarado, Elastic spin-polarized low-energy electron scattering from magnetic surfaces, in *Polarized Electrons in Surface Physics* (World Scientific, Singapore, 1986) pp. 321–352.

[42] H.-J. Elmers, Spin-polarized low energy electron diffraction, 10.1002/9780470022184.hmm307 (2007).

[43] Y. Zhang, P. A. Ignatiev, J. Prokop, I. Tudosa, T. R. F. Peixoto, W. X. Tang, K. Zakeri, V. S. Stepanyuk, and J. Kirschner, Elementary excitations at magnetic surfaces and their spin dependence, Phys. Rev. Lett. **106**, 127201 (2011).

[44] K. Zakeri and C. Berthod, Theory of spin-polarized high-resolution electron energy loss spectroscopy from nonmagnetic surfaces with a large spin-orbit coupling, Phys. Rev. B **106**, 235117 (2022).

[45] M. Plihal, D. L. Mills, and J. Kirschner, Spin wave signature in the spin polarized electron energy loss spectrum of ultrathin fe films: Theory and experiment, Phys. Rev. Lett. **82**, 2579 (1999).

[46] K. Zakeri and J. Kirschner, *Probing Magnons by Spin-Polarized Electrons* (Springer, Berlin, Heidelberg, 2013), Chap. 7, pp. 84–99.

[47] K. Zakeri, Elementary spin excitations in ultrathin itinerant magnets, Phys. Rep. **545**, 47 (2014).

[48] See Supplemental Material at http://link.aps.org/supplemental/10.1103/PhysRevLett.132.126702, which includes Refs. [22,23,26,39,40,44–47,49–65], for detailed information.

[49] I. Dzyaloshinsky, A thermodynamic theory of weak ferromagnetism of antiferromagnetics, J. Phys. Chem. Solids **4**, 241 (1958).

[50] T. Moriya, Anisotropic superexchange interaction and weak ferromagnetism, Phys. Rev. **120**, 91 (1960).

[51] L. Udvardi and L. Szunyogh, Chiral asymmetry of the spin-wave spectra in ultrathin magnetic films, Phys. Rev. Lett. **102**, 207204 (2009).

[52] A. T. Costa, R. B. Muniz, S. Lounis, A. B. Klautau, and D. L. Mills, Spin-orbit coupling and spin waves in ultrathin ferromagnets: The spin-wave Rashba effect, Phys. Rev. B **82**, 014428 (2010).

[53] K. Zakeri, Probing of the interfacial Heisenberg and Dzyaloshinskii–Moriya exchange interaction by magnon spectroscopy, J. Phys. Condens. Matter **29**, 013001 (2017).

[54] K. Zakeri, A. Marmodoro, A. von Faber, S. Mankovsky, and H. Ebert, Chirality-inverted Dzyaloshinskii-Moriya interaction, Phys. Rev. B **108**, L100403 (2023).

[55] K. Zakeri, D. Rau, J. Jandke, F. Yang, W. Wulfhekel, and C. Berthod, Direct probing of a large spin-orbit coupling in the FeSe superconducting monolayer on STO, ACS Nano **17**, 9575 (2023).

[56] J. Kirschner, Direct and exchange contributions in inelastic scattering of spin-polarized electrons from iron, Phys. Rev. Lett. **55**, 973 (1985).

[57] K. Zakeri, J. Wettstein, and C. Sürgers, Generation of spin-polarized hot electrons at topological insulators surfaces by scattering from collective charge excitations, Commun. Phys. **4**, 225 (2021).

[58] M. P. Gokhale, A. Ormeci, and D. L. Mills, Inelastic scattering of low-energy electrons by spin excitations on ferromagnets, Phys. Rev. B **46**, 8978 (1992).

[59] M. P. Gokhale and D. L. Mills, Spin excitations of a model itinerant ferromagnetic film: Spin waves, Stoner excitations, and spin-polarized electron-energy-loss spectroscopy, Phys. Rev. B **49**, 3880 (1994).

[60] Y. Zhang, T.-H. Chuang, K. Zakeri, and J. Kirschner, Relaxation time of terahertz magnons excited at ferromagnetic surfaces, Phys. Rev. Lett. **109**, 087203 (2012).

[61] H. J. Qin, K. Zakeri, A. Ernst, L. M. Sandratskii, P. Buczek, A. Marmodoro, T. H. Chuang, Y. Zhang, and J. Kirschner, Long-living terahertz magnons in ultrathin metallic ferromagnets, Nat. Commun. **6**, 6126 (2015).

[62] A. Lucas and M. Šunjić, Fast-electron spectroscopy of collective excitations in solids, Prog. Surf. Sci. **2**, 75 (1972).

[63] P. Lambin, J.-P. Vigneron, and A. Lucas, Computation of the surface electron-energy-loss spectrum in specular geometry for an arbitrary plane-stratified medium, Comput. Phys. Commun. **60**, 351 (1990).

[64] M. A. Ordal, L. L. Long, R. J. Bell, S. E. Bell, R. R. Bell, R. W. Alexander, and C. A. Ward, Optical properties of the

metals Al, Co, Cu, Au, Fe, Pb, Ni, Pd, Pt, Ag, Ti, and W in the infrared and far infrared, Appl. Opt. **22**, 1099 (1983).
[65] W. E. Vargas, F. Muoz-Rojas, E. Avendao, V. Quirós-Cordero, and M. Hernández-Jiménez, Optical, charge transport, thermal, magnetic, plasmonic, and quantum mechanical properties of iridium, Recent Prog. Mater. **04**, 1 (2022).
[66] R. Vollmer, M. Etzkorn, P. S. A. Kumar, H. Ibach, and J. Kirschner, Spin-polarized electron energy loss spectroscopy of high energy, large wave vector spin waves in ultrathin FCC Co films on Cu(001), Phys. Rev. Lett. **91**, 147201 (2003).
[67] R. Vollmer, M. Etzkorn, P. S. A. Kumar, H. Ibach, and J. Kirschner, Spin-wave excitation observed by spin-polarized electron energy loss spectroscopy: A new method for the investigation of surface- and thin-film spin waves on the atomic scale, Thin Solid Films **464–465**, 42 (2004).
[68] M. Etzkorn, P. S. Anil Kumar, R. Vollmer, H. Ibach, and J. Kirschner, Spin waves in ultrathin Co-films measured by spin polarized electron energy loss spectroscopy, Surf. Sci. **566–568**, 241 (2004).
[69] K. Zakeri, T.-H. Chuang, A. Ernst, L. Sandratskii, P. Buczek, H. Qin, Y. Zhang, and J. Kirschner, Direct probing of the exchange interaction at buried interfaces, Nat. Nanotechnol. **8**, 853 (2013).
[70] K. Zakeri, H. Qin, and A. Ernst, Unconventional magnonic surface and interface states in layered ferromagnets, Commun. Phys. **4**, 18 (2021).
[71] A. K. Geim and I. V. Grigorieva, van der Waals heterostructures, Nature (London) **499**, 419 (2013).
[72] K. S. Novoselov, A. Mishchenko, A. Carvalho, and A. H. C. Neto, 2D materials and van der Waals heterostructures, Science **353**, 461 (2016).
[73] Y. Liu, N. O. Weiss, X. Duan, H.-C. Cheng, Y. Huang, and X. Duan, Van der Waals heterostructures and devices, Nat. Rev. Mater. **1**, 16042 (2016).
[74] J. G. Rau, E. K.-H. Lee, and H.-Y. Kee, Spin-orbit physics giving rise to novel phases in correlated systems: Iridates and related materials, Annu. Rev. Condens. Matter Phys. **7**, 195 (2016).
[75] A. K. Kundu, *Magnetic Perovskites* (Springer, India, 2016).
[76] I. Razdolski, A. Alekhin, N. Ilin, J. P. Meyburg, V. Roddatis, D. Diesing, U. Bovensiepen, and A. Melnikov, Nanoscale interface confinement of ultrafast spin transfer torque driving non-uniform spin dynamics, Nat. Commun. **8**, 15007 (2017).
[77] M. L. M. Lalieu, R. Lavrijsen, R. A. Duine, and B. Koopmans, Investigating optically excited terahertz standing spin waves using noncollinear magnetic bilayers, Phys. Rev. B **99**, 184439 (2019).
[78] D. C. Tsui, R. E. Dietz, and L. R. Walker, Multiple magnon excitation in NiO by electron tunneling, Phys. Rev. Lett. **27**, 1729 (1971).
[79] J. S. Moodera, J. Nowak, and R. J. M. van de Veerdonk, Interface magnetism and spin wave scattering in ferromagnet-insulator-ferromagnet tunnel junctions, Phys. Rev. Lett. **80**, 2941 (1998).
[80] J. Murai, Y. Ando, M. Kamijo, H. Kubota, and T. Miyazaki, Direct observation of magnon excitation in a ferromagnetic tunnel junction using inelastic-electron-tunneling spectroscopy, Jpn. J. Appl. Phys. **38**, L1106 (1999).
[81] G. D. Fuchs, N. C. Emley, I. N. Krivorotov, P. M. Braganca, E. M. Ryan, S. I. Kiselev, J. C. Sankey, D. C. Ralph, R. A. Buhrman, and J. A. Katine, Spin-transfer effects in nanoscale magnetic tunnel junctions, Appl. Phys. Lett. **85**, 1205 (2004).
[82] T. Balashov, A. F. Takács, W. Wulfhekel, and J. Kirschner, Magnon excitation with spin-polarized scanning tunneling microscopy, Phys. Rev. Lett. **97**, 187201 (2006).
[83] O. Dzyapko, H. Kurebayashi, V. E. Demidov, and S. O. Demokritov, Control of pure spin current by magnon tunneling and three-magnon splitting in insulating yttrium iron garnet films, in *Recent Advances in Magnetic Insulators—From Spintronics to Microwave Applications* (Elsevier, New York, 2013), pp. 83–122.
[84] D. Ghazaryan, M. T. Greenaway, Z. Wang, V. H. Guarochico-Moreira, I. J. Vera-Marun, J. Yin, Y. Liao, S. V. Morozov, O. Kristanovski, A. I. Lichtenstein, M. I. Katsnelson, F. Withers, A. Mishchenko, L. Eaves, A. K. Geim, K. S. Novoselov, and A. Misra, Magnon-assisted tunnelling in van der Waals heterostructures based on $CrBr_3$, Nat. Electron. **1**, 344 (2018).